The Research Council of Norway (NFR)

NORSAR

NORSAR Scientific Report No. 2-97/98

Semiannual Technical Summary

1 October 1997 – 31 Mars 1998

Kjeller, May 1998

7 Summary of Technical Reports / Papers Published

7.1 Seismic Threshold Monitoring for continuous assessment of Global detection capability

Summary

Continuous seismic threshold monitoring is a technique that has been developed over the past several years to use a seismic network for monitoring a geographical area continuously in time. The method provides, at a given confidence level, a continuous assessment of the upper magnitude limit of possible seismic events that might have occurred in the target area. In this paper we expand upon previous work to apply the method to a global network of seismic stations, and give examples of application from a prototype system which will eventually be installed at the International Data Center for monitoring the comprehensive nuclear test ban treaty.

Using a global grid of 2562 geographical aiming points, we compute site-specific threshold traces for each grid point, and apply spatial interpolation to obtain full global coverage. For each grid point, the procedure is in principle to "focus" the network by tuning the frequency filters and array beams using available information on signal and noise characteristics at each station-site combination. Generic phase attenuation relationships and standard travel-time tables are used in this initial implementation, but the system lends itself easily to applying station-site specific corrections (magnitudes, travel-times, etc.) to each seismic phase.

We give examples of two main types of applications based on data from a world-wide seismic network: a) an estimated continuous *global threshold level* and b) an estimated continuous *global detection capability.* The first application provides a continuous view of the global seismic "background field" as calculated from the station data, with the purpose to assess the upper magnitude limit of any seismic event that might have occurred around the globe. The second application introduces detection thresholds for each station and provide a simplified estimate, continuously in time, of the n-station detection capability of the network. The latter approach naturally produces higher threshold values, with the difference typically being 0.5-1 magnitude unit. We show that both these approaches are useful especially during large earthquakes, where conventional capability maps based on statistical noise and signal models cannot be applied.

In order to illustrate the usefulness of combining the global monitoring with site-specific monitoring for areas of special interest, we consider a large earthquake aftershock sequence in Kamchatka and its effect on the threshold trace in a very different region (the Novaya Zemlya nuclear test site). We demonstrate that the effects of the aftershock signals on the thresholds calculated for Novaya Zemlya are modest, partly due to the emphasis on high-frequency signals. This indicates that threshold monitoring could provide significantly improved event detection during aftershock sequences compared to conventional methods, for which the large number of detected phases tends to cause problems in the phase association process.

Introduction

Traditionally, assessments of seismic network detection capabilities are based upon assuming statistical models for the noise and signal distributions. These models include station correc-

tions for signal attenuation and a combinational procedure to determine the detection threshold as a function of the number of phase detections required for reliable location (Sykes & Evernden 1982; Harjes, 1985; Hannon 1985; Ringdal 1986; Sereno & Bratt, 1989).

In general, it is implicitly understood that any network will have a detection threshold that varies with time. It is important to retain such information along with the information on the average capability. However, with methods being used in practical operation today, no attempt is made to specify the time-dependency of the calculated threshold. For example, the noise models used in these capability assessments are not able to accommodate the effect of interfering signals, such as the coda of large earthquakes, which may cause the estimated thresholds to be significantly degraded at times. Furthermore, only a statistical capability assessment is achieved, and no indication is given as to particular time intervals when the possibility of undetected seismic events is particularly high, for example during unusual background noise conditions or outages of key stations.

The continuous threshold monitoring technique has been developed to address these problems. The basic principles were described by Ringdal & Kværna (1989, 1992), who showed that this method could be useful as a supplement to event detection analysis. In this paper we expand further on the utility of this method, with particular emphasis on seismic threshold monitoring on a global scale, using a world-wide network. Some examples are given on how such monitoring could be achieved in a practical system, which will eventually be implemented at the International Data Center for monitoring a Comprehensive Test Ban Treaty (CTBT).

Approaches to threshold monitoring

The capability achieved by the threshold monitoring method is in general dependent upon the size of the target area, and it is convenient to consider three basic approaches:

Site-specific threshold monitoring: A seismic network is focused on a small area, such as a known test site. This narrow focusing enables a high degree of optimization, using site-station specific calibration parameters and sharply focused array beams.

Regional threshold monitoring: Using a dense geographical grid, and applying site-specific monitoring to each grid point, threshold contours for an extended region are computed through interpolation. In contrast to the site-specific approach, it is usually necessary to apply generic attenuation relations, and the monitoring capability will therefore not be quite as optimized.

Global threshold monitoring: This is a natural extension of the regional monitoring approach, but requires a somewhat different strategy for effective implementation. Using a global network, and taking into account that phase propagation time is up to several tens of minutes, it is necessary to establish elaborate global travel-time and attenuation tables, and to use a much coarser geographical grid than in the regional approach.

The regional and global monitoring techniques provide geographical threshold maps that have several advantages over standard network capability maps. They are far more accurate during time intervals when interfering seismic events occur. They can also more easily reflect special conditions such a particularly favorable source-station propagation paths, and have the advantage of not being tied to specific event detection criteria.

In this paper, an overview is given of the underlying principles for continuous threshold monitoring on a global scale.

Method description

Generating the threshold trace

Let us assume that a network of seismic stations are available for monitoring a specified target site. For simplicity of presentation, we will assume that these are all array stations, able to provide phase velocity and azimuth information for detected signals. Extension to the single-station case is straightforward. The stations can be located either at regional or teleseismic distances.

Following Ringdal & Kværna (1992), let us consider a network of seismic stations (i=1,2....,N) and a number of seismic phases (j=1,2,...,M). For a seismic event of magnitude m_b=m an estimate $\hat{m}_{ij}$ of m is given by

$$\hat{m}_{ij} = \log S_{ij} + b_j(\Delta, h) \tag{1}$$

where S_{ij} is the measured signal power of the *j-th* phase at the *i-th* station

$b_j(\Delta, h)$ is a distance-depth correction factor for the *j-th* phase.

In standard formulas for magnitude, the signal power S_{ij} is usually estimated as A/T, i.e., amplitude divided by dominant signal period. In our case, we will assume that S_{ij} is the measurement of signal power (e.g., short term average, STA) at the expected signal arrival time. The value is measured on an array beam or a single channel filtered in an appropriate frequency band.

Traditionally, the relation (1) is defined only for the time window corresponding to a detected seismic event. We will now consider the righthand side of (1) as a continuous function of time. Define the "threshold parameter" $a_{ij}(t)$ as follows:

$$a_{ij}(t) = \log S_{ij}(t) + b_j(\Delta, h) \tag{2}$$

The equation (2) represents a function which can be considered as a continuous representation of the upper magnitude limit for a hypothetical seismic event at a given geographical location (target region). It coincides with the event magnitude estimate if an event occurs at that site. The function is, by definition, tied to a specific station and a specific phase.

Using a statistical approach, and assuming statistical independence of the observations, we can now proceed as described by Ringdal and Kværna (1989). After time-aligning the threshold traces to correspond to the target area, we obtain a network-based representation of the upper magnitude limit by considering the function:

$$g(m, t) = 1 - \prod_{i,j}\left(1 - \Phi\left(\frac{(m - a_{ij}(t))}{\sigma_{ij}}\right)\right) \tag{3}$$

where m is event magnitude, σ_{ij} is the standard deviation of the assumed magnitude distribution for the i-th station and j-th phase and Φ denotes the standard (0,1) normal distribution function.

The function $g(m, t)$ is the probability that a given (hypothetical) seismic event of magnitude m at time t would generate signals that exceed the observed noise values at at least one station of the network. For a given t, the function $g(m, t)$ is a monotonously increasing function of m, with values between 0 and 1. A 90% upper limit at time t is defined as the solution to the equation

$$g(m, t) = 0.90 \tag{4}$$

The solution is a function of t, which we will denote $n_{T90}(t)$. We call this the *threshold trace* for the network and target region being considered.

Calculating a "detection capability" trace

The *threshold trace* developed above is not directly related to the *detection capability* of the network in the usual sense. Nevertheless, the general method described above can easily be used to obtain a continuous estimate of the network *n-station* detection capability. In order to do this, we must add the required signal-to-noise ratio (SNR) to each individual station threshold trace and adjust the level to correspond to a probability level of 90% for phase detection at each station. Let us denote by T_{ij} the SNR (in log units) required for detection at the *i'th* station and the *j'th* phase, and denote by $d_{ij}(t)$ the corresponding station detection threshold (in magnitude units). Further, let σ_{ij} denote the assumed standard deviation of the (hypothetical) signal. We then obtain:

$$d_{ij}(t) = a_{ij}(t) + T_{ij} + \mu_{90} \cdot \sigma_{ij} \tag{5}$$

where $\mu_{90} = 1.282$ is the 90% quantile in the standard normal distribution function. In this particular connection, let us for simplicity consider only P-type phases (the extension to the general case is obvious). Eliminating the index j, we order the individual station detection thresholds so that:

$$d_1(t) \leq d_2(t) \leq \ldots \leq d_N(t) \tag{6}$$

We define the *M-station network detection threshold* at time t as the magnitude value $d_M(t)$. For a hypothetical event at this magnitude we would then expect at least M stations to exceed their respective detection thresholds, thus allowing for a network detection of the hypothetical event.

We note that this formulation is quite different from the standard methods for network detection threshold estimation (Harjes, 1985) for several reasons:

- Standard methods assume a statistical distribution of noise and signal amplitude levels, while our approach covers the actually recorded seismic field continuously
- Standard methods employ a somewhat more complicated combinatorial technique, that we have simplified by ordering the individual station thresholds by increasing magnitude.

We can in fact apply a variant of the standard method to use the actually recorded seismic field instead of a statistical noise model. Define the detection probability $P_i(m)$ of the ith station by using the same notation as in (3), but without the time variable t and the phase index j:

$$P_i(m) = \Phi\left(\frac{(m-(a_i+T))}{\sigma_i}\right) \tag{7}$$

We assume that the probability of detection is statistically independent among the stations in the network. Setting for simplicity of notation $P_i=P_i(m)$, the probability $P(K/m)$ that exactly K out of the N station will detect the event (given its magnitude m) becomes:

$$P(K/m) = \sum_{(i_1<i_2<\cdots<i_K)} (P_{i_1})\cdot(P_{i_2})\cdot\cdots\cdot(P_{i_K}) \prod_{(j\neq i_1,i_2,\ldots,i_K)} (1-P_j) \tag{8}$$

By summing terms as above we will obtain the probability that at least M out of N stations detect the event. The 90% detection threshold for M-station detection is thus the solution of the equation:

$$1 - \sum_{K=0}^{M-1} P(K/m) = 0.90 \tag{9}$$

It would be feasible, given sufficient computer resources, to calculate the detection thresholds in this "combinatorial" way on a continuous basis by using the individual station threshold traces as input. We have found, however, by studying various examples, that our simplified calculation based on eq. (6) gives generally consistent results with such combinatorial calculations, and that the divergences are in practice in the range 0-0.2 magnitude units. This is well below the inherent uncertainties in either method. We therefore use the simplified method in presenting our continuous global network detection threshold estimates.

Applying distance-depth corrections

Let us first consider threshold monitoring of a specific target area of limited geographical extent. The size of the target area may vary depending upon the application, but typically such an area might be a few tens of kilometers in diameter. A basic assumption is that the target area is defined such that all seismic events within the area show similar wave propagation characteristics.

The distance-depth correction factors $b_j(\Delta, h)$ in (1) and (2) can either be determined by using "generic" values representative for a larger region, or by calibration to the specific target area. The latter method is the most accurate and is preferable, assuming that previous calibration events are available. We then obtain the necessary magnitude calibration factors from processing previous events with known magnitude, using the relation

$$\hat{b}_{i,j} = \hat{m}_j - \log(\hat{S}_{i,j}) \qquad (i = 1, \ldots, K;\ j = 1, \ldots, L) \tag{10}$$

where $\hat{b}_{i,j}$ is our estimate of the magnitude correction factor for phase i and event j, $\hat{m}_j$ is the estimate of the magnitude for event j (based on independent network observations), and $\hat{S}_{i,j}$ is our estimate of the signal level at the predicted arrival time of phase i for event j. K is the num-

ber of phases considered (there might be several stations and several phases per station), and L is the number of events.

The magnitude correction factor to be used for phase i is then given by

$$b_i = \frac{1}{L} \cdot \sum_{j=1}^{L} \hat{b}_{i,j} \tag{11}$$

Parameters such as window lengths for signal level estimation, travel-times of the different phases, filter frequency bands and steering delays for array beamforming are obtained on the basis of processing results for the calibration events.

Developing a global grid

In principle, global threshold monitoring can be achieved by conducting site-specific monitoring of a grid of target points covering the globe. The density of the grid and the interpolation technique applied will determine the quality of the results.

We have adopted the method described by Vinje et al (1992) to develop global grid point systems. This method applies triangulation of an icosahedron to construct regularly sampled wavefronts, and provides close to uniform geographical coverage of the globe at a specified grid density (Kværna, 1992).

The grid density to be used in practice is mainly a cost-performance trade-off. We have chosen a 2562-point grid for the initial version of a global threshold monitoring system. This grid is shown in Figure 1, and corresponds to a radius of approximately 2.7 degrees for the area covered by each grid point.

It is important to be aware that the density of the global grid is quite different from the beam deployment density for the arrays in the station network. For each array, a certain number of steering points will be selected (typically a few tens for a small or medium aperture array, and more than 100 for a large array). When calculating the threshold traces for a given global grid point, the closest beam steering point is selected. Thus, there will be a potential beam steering loss that must be taken into account when calculating the "representative" threshold for the area represented by the global grid point.

The beam steering loss is mainly a function of array aperture and signal frequency. An illustration for the ASAR array is given in Figure 2, showing 3 dB beam loss contours for the selected filter band for that array (1.0-4.5Hz). These loss contours are circles when shown in inverse velocity space, and the steering points therefore do not translate into equidistant geographical points. Thus, if mainly teleseismic distances are considered, the number of steering points for a given worst-case loss will be modest. In our calculations, we have set the beam density in such a way that the maximum expected missteering loss is 3dB.

Calibration and time/azimuth tolerances

Ideally, global threshold monitoring requires access to magnitude calibration statistics for each target point and each station/phase combination considered. In a practical situation it will usually be impossible to obtain the necessary number of calibration events for each target point in the grid, and a different approach is therefore required.

Our approach is to develop a set of "generic" attenuation models. This can be done as a two-step process. The first step is to divide the earth into regions that are relatively homogeneous with respect to wave propagation characteristics. Within each region, an attenuation model is then established on the basis of available calibration data.

Using this approach, the distance-depth correction factors $b(\Delta, h)$ in (1) can be determined individually for each seismic phase, by applying a standard global attenuation model, in combination with region-specific station corrections.

In threshold monitoring there is a trade-off between the size of the target area and the tolerances of the parameter values used in the threshold computations. With a given grid, it is necessary to make the tolerances of each aiming point compatible with the grid spacing.

An illustration of the time and azimuth tolerances is given in Kværna et. al. (1994). For example, if we increase the time windows over which we measure the signal levels, this has the effect of broadening the target area for the aiming point. At the same time, some of the resolution in the regional threshold variation will be lost. The necessary time window corresponding to a typical teleseismic distance is of the order of ± 1 minute. A similar consideration applies to azimuth and slowness tolerances.

Parameter settings

General considerations

The basic components in global threshold monitoring are the stations in the network and the set of grid points. A station can be an array, a three-component station or a single-component station. The type of seismometer, digitizer, sampling rate and response function can vary, although for the purpose described here we will restrict ourselves to the short period processing band (typically 0.5 Hz and higher). A grid point is an aiming point in geographical space.

In global threshold monitoring, the number of grid points and their density and distribution may vary according to the available network, the monitoring requirements and the computing facilities available.

For each station, the following information is required:

- Latitude, longitude, height
- Types and deployments of sensors
- System response
- Sampling rate
- Number of beams
- Beam steering points and filter bands
- STA lengths and update rates

For each station/grid point combination, the following information is required:

- Latitude, longitude, depth
- Grid spacing
- A phase type indicator for each phase used
- Pointers to the nearest beams

- Station-site specific corrections if available (magnitude, travel-time etc.)

Beam deployment

The beam deployment is made taking into account the need for regional characterization (for non-arrays as well as arrays) and the allowable worst-case beam loss for the appropriate regional coverage. The beam configurations are set so as to obtain the optimum SNR for the actual beam in the frequency band used. The SNR is defined as the signal strength relative to the normal noise conditions.

Filter bands

The filter bands are set for each grid point-station-phase combination and should be designed for optimum SNR for all events of interest in the area covered by the grid point. Initially, we use a set of generic, wide-band filters, typically 0.8-4.5 Hz, but usually with higher frequency bands at local and regional distances (Kvœrna, 1996). Furthermore, the selection of filter band also depends upon the typical signal and noise spectra at the station. The filter bands will be refined on an individual station basis as experience accumulates.

STA calibration

Since STA values are used instead of A/T as a basis for magnitude estimates, it is necessary to introduce a conversion formula. From experiments with different short-period instrument types, we have found that such a relation can be well parameterized in the following way:

$$\log(A/T) \approx \log((\pi/2)STA \times cal_{1.0}) + c(resp, filter) \tag{12}$$

where $cal_{1.0}$ is the instrument calibration factor at 1 Hz, and c is a constant that is dependent on the instrument response and the filter band used to calculate the STA value (Kvœrna, 1996). The constant c is derived empirically for each instrument and the filter band, as illustrated in Figure 7.1.3.

Initial IDC implementation

The initial IDC implementation comprises the following main features:

- Continuous global detection capability map
- 2562 grid points
- 10 seconds update rate
- 7-day diskloop of STA values and capability maps
- Hourly summaries of station availability and background noise levels
- Hourly average and worst-case global capability maps

Provision for extracting site-specific traces will be implemented as a future option. It should be noted that such site-specific traces will initially be represented by the trace of the closest global grid point. "Optimum" site-specific traces could later be generated for regions where sufficient calibration information is available, as we will show in an example later.

Analysis results

Based on the raw data, three sets of results are generated by the automatic global threshold monitoring system on an hourly basis. These quantify both the network detection capability of the primary seismic network for monitoring the CTBT, and provide information on factors causing a possible degradation of this detection capability. A set of results from the TM system, describing the network detection capability for the one-hour interval 1998/05/11 10:00 to 11:00 is given in the following:

- The first set of results, (see example in Section 7.2, Figure 7.2.2), provides information on the data availability and interfering events for the particular 1-hour interval. The color of the station symbols provide information on the availability of data for a particular 1-hour interval (1998/05/11 10:00 to 11:00). The arrays are marked by circles and three-component stations by triangles. Notice that for the interval reported, several of the stations were out of operation for all or part of the time. The locations of events in the Reviewed Event Bulletin (REB) during the actual time interval are plotted, and the event information is given below the map. Notice the occurrence of the Indian nuclear explosion (m_b 5.0)
- The second set of results (see example in Section 7.2, Figure 7.2.3) is an overview of the background noise level and the observed signals at each of the primary stations during the data interval (1 hr 22 min 20 s) used for assessing the detection capability of the 1 hour interval. The traces shown are continuous log (A/T) equivalents derived from the STA traces. Notice in particular the signals from the m_b 5.0 event in India (origin time 10:13:44) seen at most stations of the primary network. The percentages of successfully recorded and processed data are also given for each station, and the intervals with gaps in data processing are indicated in red above the time axis.
- The third set of results (see example in Section 7.2, Figure 7.2.4), is a periodic capability map. The upper map of the figure shows the average network detection capability for the 1-hour interval (1998/05/11 10:00 to 11:00). Variation from hour to hour of the average detection capability is primarily caused by longer station or processing outages, by increased background noise levels at the different stations, or by signals of long duration from large seismic events. The lower map shows the worst-case detection capability for the analyzed hour. Differences from the average capability are primarily caused by signals from seismic events, short outages and data quality problems. Notice that the m_b 5.0 event in India temporarily causes a degradation of the detection capability all over the world, and in particular in the vicinity of the actual event location.

Both types of maps shown in Section 7.2, Figure 7.2.4 provide important information on the capability of the primary seismic network to detect events in different parts of the world, and the information provided in Section 7.2, Figures 7.2.2 and 7.2.3 will help to explain the variations in the global event detection capability.

The sets of results provided by the global threshold monitoring system are in this way useful for assessing the performance of the International Monitoring System, and also by giving a warning in the case of lowered monitoring capability, e.g., caused by station outages, communication problems, data processing problems or extremely high seismic activity.

Figure 7.1.4 illustrates the two different approaches to describe the global seismic field using as an example a snapshot of the threshold levels during a time without significant seismic activity:

- *Global threshold level:* The top part of Figure 7.1.4 displays the "global threshold level" for the time instance considered. We recall that this level describes the "background seismic field", with no allowance made for station detection thresholds and no requirement for station detection. The map thus shows the actually observed seismic field as seen by the network.
- *Global detection capability:* The bottom part of Figure 7.1.4 corresponds to the 3-station detection capability for the time instance considered. Note that the levels are considerably higher than in the top part of the figure, with the difference exceeding one full magnitude unit in some cases. This shows that the two approaches, although quite similar in many aspects, complement each other and provide information that could be useful in different ways.

Figure 7.1.5 illustrates the variation in global detection capability before and during a large earthquake. Four snapshots of the global detection capability of the network are shown, using a requirement of at least 3 detecting stations. There is a significant increase in the threshold levels at the time of the event, first locally and later spreading out to cover the entire world. After about 30 minutes (not shown in the figure), the levels are back to "normal".

Figure 7.1.6 shows an example of how the site-specific threshold monitoring technique can be used to supplement the global monitoring during a large earthquake followed by a large aftershock sequence. The figure shows threshold traces steered toward the Novaya Zemlya Test Site using the four IMS arrays ARCES, NORES, FINES and SPITS for the day 5 December, 1997. That day, a large (MS 7.7) earthquake occurred near E. coast of Kamchatka, followed by a very large aftershock sequence (at least 200 aftershocks during the first 12 hours detected teleseismically). There were also many "foreshocks" preceding this event. The plot shows the individual P-phases (STA traces) for each of the four arrays, with the combined network threshold monitoring trace on top. The network trace includes P and S on SPITS and ARCES, P for FINES and P for NORES. The individual arrays have large numbers of peaks corresponding to these aftershocks, whereas the network threshold trace is almost unaffected by the aftershock sequence. This shows that, when using the threshold monitoring technique, the Novaya Zemlya monitoring capability remains about the same if a large earthquake sequence occurs at a place far from the test site. We should note, however, that such good performance would not have been achieved if the sequence had taken place near the target area to be monitored.

We also add that the excellent capability of the site-specific technique as demonstrated above is due, to a large part, to our emphasis on high-frequency passbands in the regionally based site-specific monitoring. In fact, the advantages of our approach can be seen as being caused by three main factors:

- Large earthquakes tend to have predominantly low frequency energy. The resulting inincrease in the background "seismic field" is therefore much larger at frequencies around 1 Hz than at frequencies in the range 4 Hz and above. This means that stations recording high-frequency signals will be less affected by the interfering signals from such earthquakes.

- The coda of a large earthquake tends to last for several minutes in the short period band (and much longer for long period (20 seconds) signals), thus degrading the global detection capability for an extended period of time. The coda dropoff is much faster at higher frequencies, as shown by an example in Figure 7.1.7. This adds to the effect described above as far as improving the event detection capability in the earthquake coda is concerned.
- High-frequency arrays as used in our example from Novaya Zemlya have the added advantage of suppressing the noise (or signal coda) from interfering events, and retain signal coherency even at high frequencies. This further adds to the capability of detecting small events in the background of a large earthquake.

Discussion

The continuous threshold monitoring technique represents a new approach toward achieving reliable seismic monitoring. The method is well suited to supplement the traditional methods in monitoring potential test sites for the purpose of verifying a comprehensive nuclear test ban treaty. The method may equally well be used to monitor earthquake activity at low magnitudes for sites of special interest, and could also be useful for monitoring earthquake aftershock sequences. The system described here is intended to demonstrate how the concept is used in practice to enable threshold monitoring on a global basis, with applications to real-time displays.

The fact that the coda of a large earthquake tends to last for several minutes in the short period band, and much longer for long period (20 seconds) signals, has traditionally caused a significant degradation of the global detection capability of existing global networks (Bache and Bratt, 1985). While this problem cannot be entirely eliminated, we have shown that the threshold monitoring technique holds promise to reduce the adverse effects on the global detection capability. Further improvements might be achievable by extensive calibration, systematic utilization of regional networks and emphasis on the high-frequency passbands.

In principle, the global method, given enough calibration data and computer resources, could be expanded to approach the capability of the site-specific method for each target point. However, in practice, there will be a need to apply both methods in day-to-day monitoring. Another consideration here is that the site-specific method could be further optimized e.g. by considering different filter bands in parallel and applying specially generated digital filters to search for signals conforming to predetermined characteristics. We are currently investigating the feasibility and benefits of this type of optimization.

It is important to be aware that the main purpose of the threshold monitoring method is to call attention to any time instance when a given threshold is exceeded. This will enable the analyst to focus his efforts on those events that are truly of interest in a monitoring situation. He will then apply other, traditional analysis tools in detecting, locating and characterizing the source of the disturbance. Thus, the threshold monitoring method is a supplement to, and not a replacement of, traditional methods.There are four main factors that cause variations in the event detectability of the primary seismic network. These are:

- Fluctuations with time in the background noise level
- Changes in data quality at the IDC caused by communications problems, station outages or other data errors like spikes and gaps

- Temporary deficiencies in the IDC data processing
- Signals from interfering seismic events around the world.

Traditional methods for assessing the network detection capability use statistical models for the noise and signal distributions to calculate the detection thresholds as a function of the number of phase detections required for defining an event (Sykes & Evernden 1982; Harjes, 1985; Hannon 1985; Ringdal 1986; Sereno & Bratt, 1989). The noise models used in these capability assessments are not able to accommodate the effect of interfering signals, such as the coda of large earthquakes, which may cause the estimated thresholds to be quite unrealistic at times. Neither can these methods include effects like communication problems and data processing deficiencies.

The threshold monitoring approach incorporates all of the effects listed above, and will provide a valuable supplement to conventional techniques in the assessment of the detection capability of a global seismic network.

As discussed by Ringdal and Kværna (1992), continuous threshold monitoring offers a valuable supplement to traditional seismic techniques used in nuclear test ban monitoring. The method may also be useful for monitoring earthquake activity at low magnitudes for sites of special interest, as well as for monitoring earthquake aftershock sequences.

We will be continuing this study in order to characterize the long-term capabilities of the TM method for global and site-specific monitoring. At the same time, we are working on a streamlining and optimization of the technique, that should improve the performance further. These efforts will be documented in detail in a separate paper.

Acknowledgement

This research has been sponsored by the Nuclear Treaty Programs Office of the U.S. Department of Defense and monitored by the Air Force Technical Applications Center under contract no. F08650-96-C-0001.

Tormod Kværna
Frode Ringdal

References

Bache, T.C. and S.R. Bratt (1985): High frequency P-wave attenuation and degradation of detection capability by large earthquakes, *Report No. AFGL-TR-85-0211*, SAIC, San Diego, California.

Hannon, W. (1985): Seismic verification of a comprehensive test ban, *Science*, 227, 251-257.

Harjes. H.-P. (1985): Global seismic network assessment for teleseismic detection of underground nuclear explosions, *J. Geophys., 57, 1-13.*

Kværna, T. (1991): Initial development of generic relations for regional threshold monitoring, *Semiannual Tech. Summ., 1 Apr - 30 Sep 1990*, NORSAR Sci. Rep. 1-90/91, NORSAR, Kjeller, Norway.

Kværna, T. (1992): Initial results from global Generalized Beamforming, *Semiannual Tech. Summ., 1 Apr - 30 Sep 1992*, NORSAR Sci. Rep. 1-92/93, NORSAR, Kjeller, Norway.

Kværna, T. (1996): Tuning of processing parameters for Global Threshold Monitoring at the IDC, *Semiannual Tech. Summ., 1 Apr - 30 Sep 1996*, NORSAR Sci. Rep. 1-96/97, NORSAR, Kjeller, Norway.

Ringdal, F. (1986): Study of magnitudes, seismicity and earthquake detectability using a global network, *Bull. Seism. Soc. Am.*, 76, 1641-1659.

Ringdal, F. & T. Kværna (1989): A multichannel processing approach to real time network detection, phase association and threshold monitoring, *Bull. Seism. Soc. Am.*, 79, 1927-1940.

Ringdal, F. & T. Kværna (1991): Continuous threshold monitoring using "regional threshold displays", *Semiannual Tech. Summ., 1 Oct 90 - 31 Mar 91*, NORSAR Sci. Rep. 2-90/91, NORSAR, Kjeller, Norway.

Ringdal, F. & T. Kværna (1992): Continuous seismic threshold monitoring, *Geophys. J. Int.*, 111, 505-514.

Sereno, T.J. & S.R. Bratt (1989): Seismic detection capability at NORESS and implications for the detection threshold of a hypothetical network in the Soviet Union, *J. Geophys. Res.*, 94, 10397-10414.

Sykes, L. & J. Evernden (1982): The verification of a comprehensive nuclear test ban, *Sci. Am.*, 247, 47-55.

Vinje, V., E. Iversen, H. Gjøystdal & K. Åstebøl (1992): Traveltime and amplitude estimation using wavefront construction. Abstract of paper presented at the 54th Meeting and Technical Exhibition of the European Association of Exploration Geophysicists, Paris, France, 1-5 June 1992.

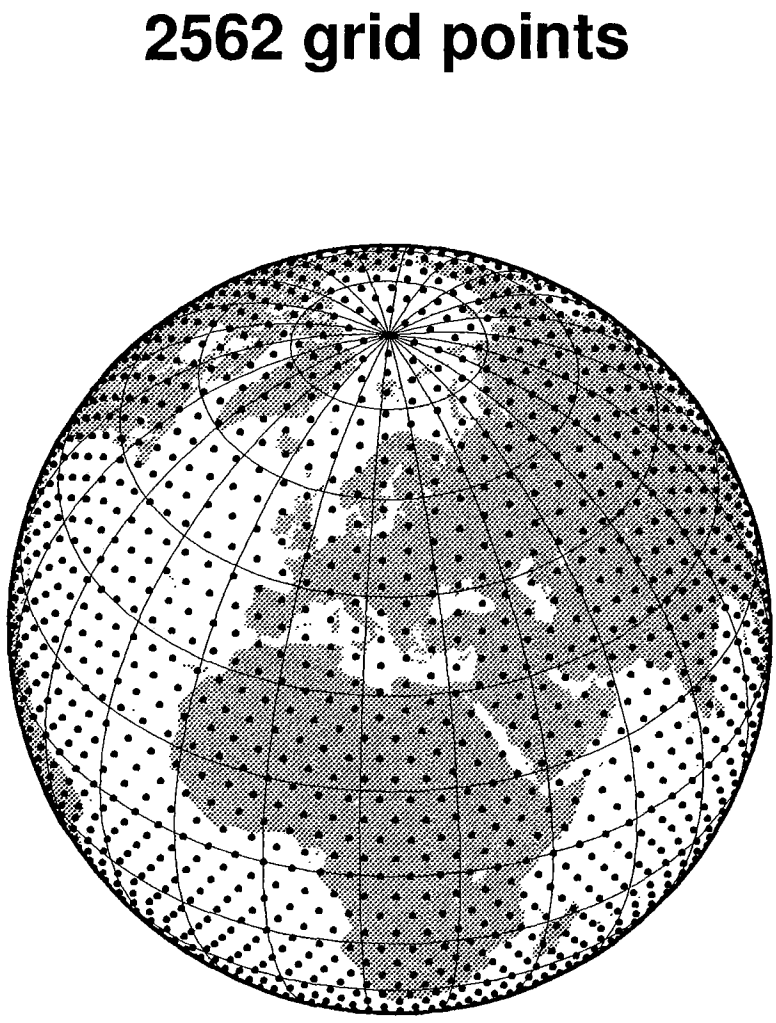

Fig. 7.1.1. The global threshold monitoring is based on a grid of 2562 target points projected upon an azimuthal orthographic projection of the earth. The grid was obtained by a four-fold triangulation of the icosaeder, and each grid point represents a target region of 2.7 degrees radius.

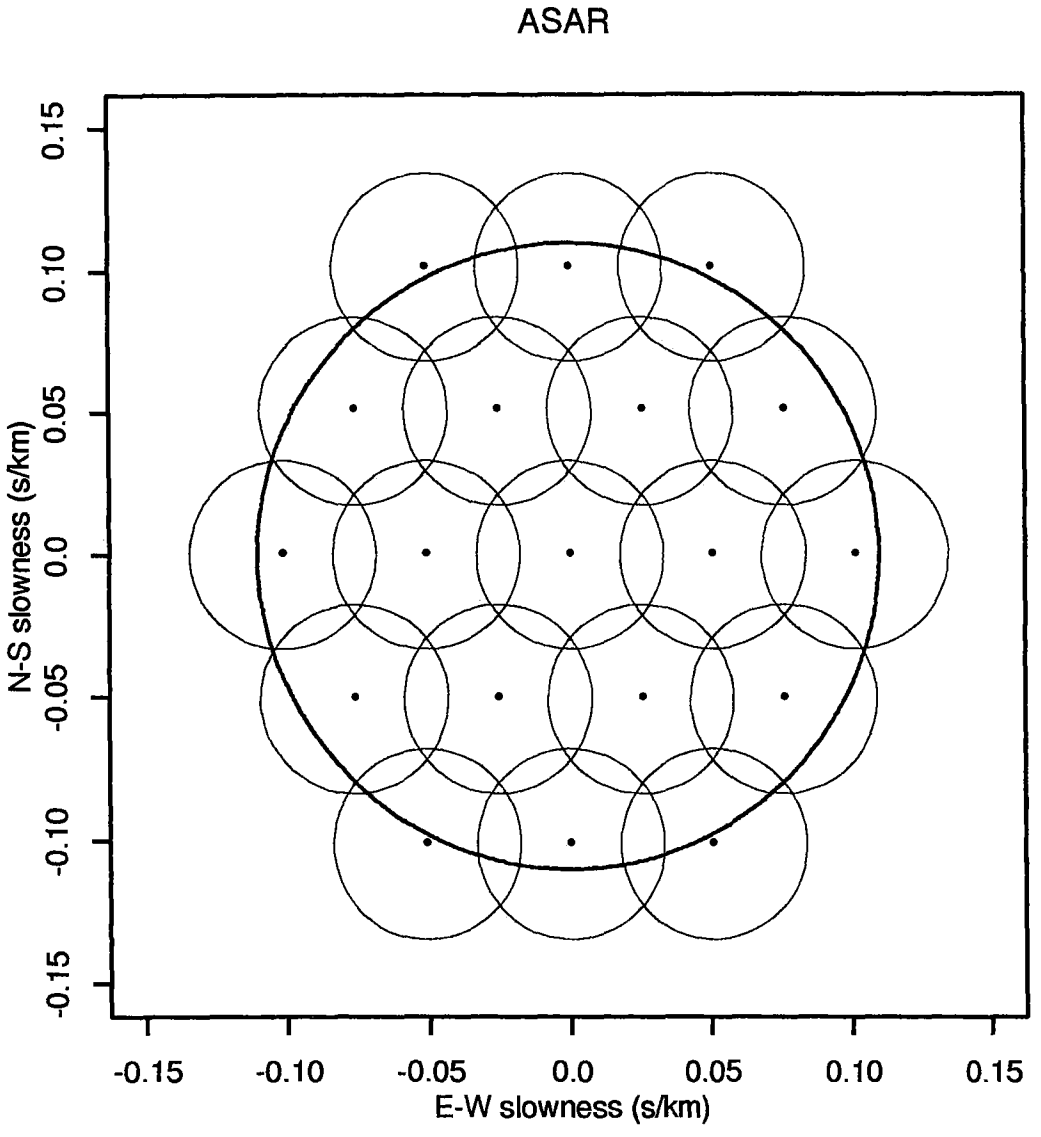

Fig. 7.1.2. Beam deployment for the ASAR array used in the threshold monitoring calculations. The circles around each beam point correspond to 3 dB beam loss contours. The beam density has been determined based upon a reference data set filtered in the frequency band 1.0-4.5 Hz.

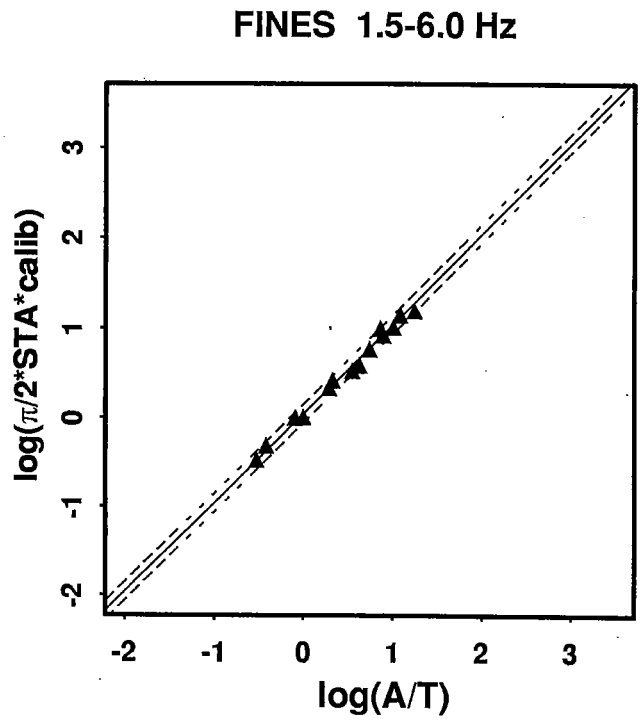

Fig. 7.1.3. Illustration of the linear relation between log(A/T) and log(STA(calibrated)) for the IMS station FINES. The straight line has been fitted with a restricted slope of 1.0, and shows an excellent correspondence with the data points.

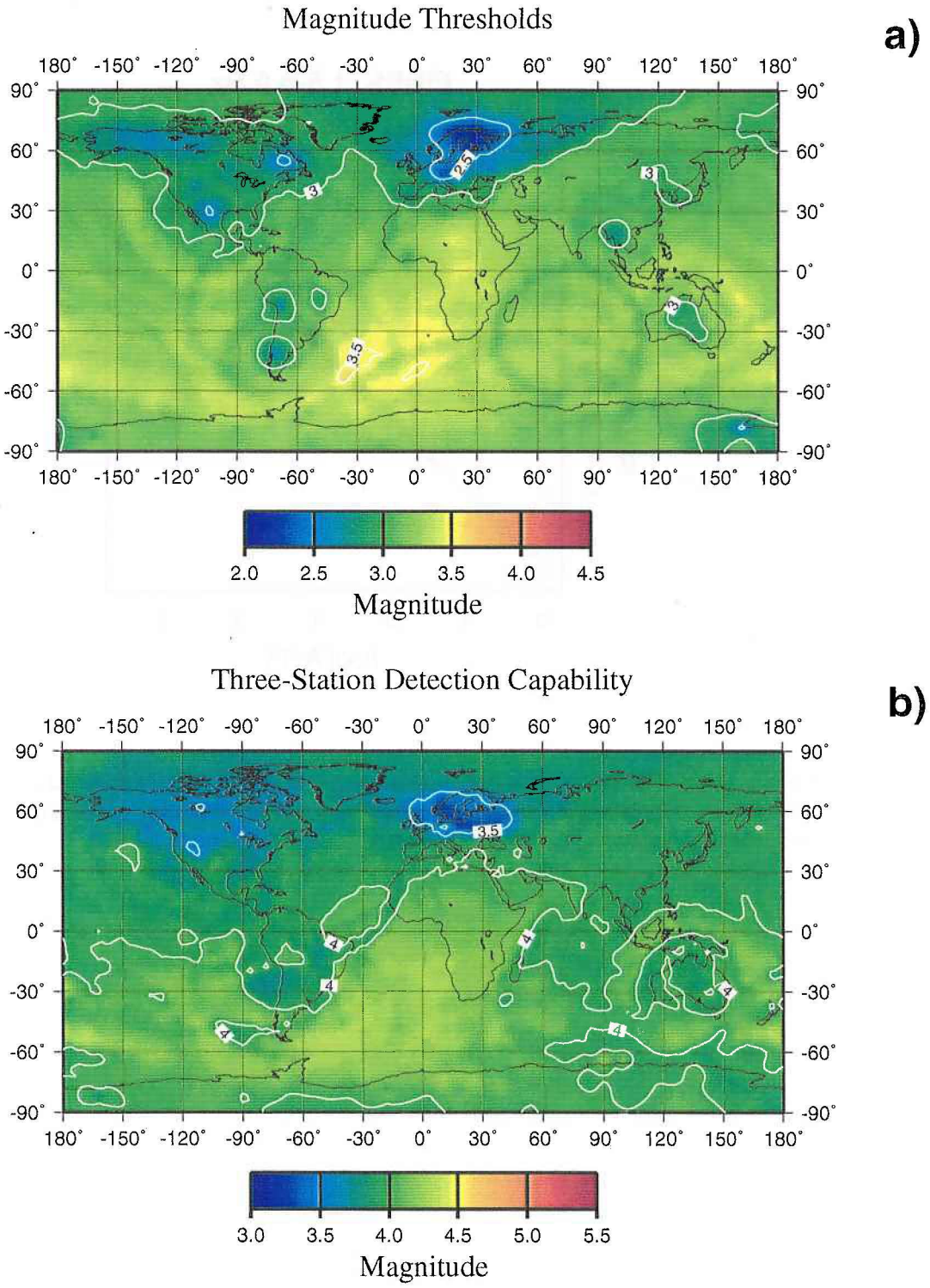

Fig. 7.1.4. Snapshots of the network global thresholds (top) and 3-station detection capability (bottom) during a time without significant seismic activity. The global threshold map shows levels about one magnitude unit lower than the detection capability map (note the difference in color codings). The bottom figure is comparable to the traditional 3-station global capability maps, since it essentially represents detection capability during noise conditions.

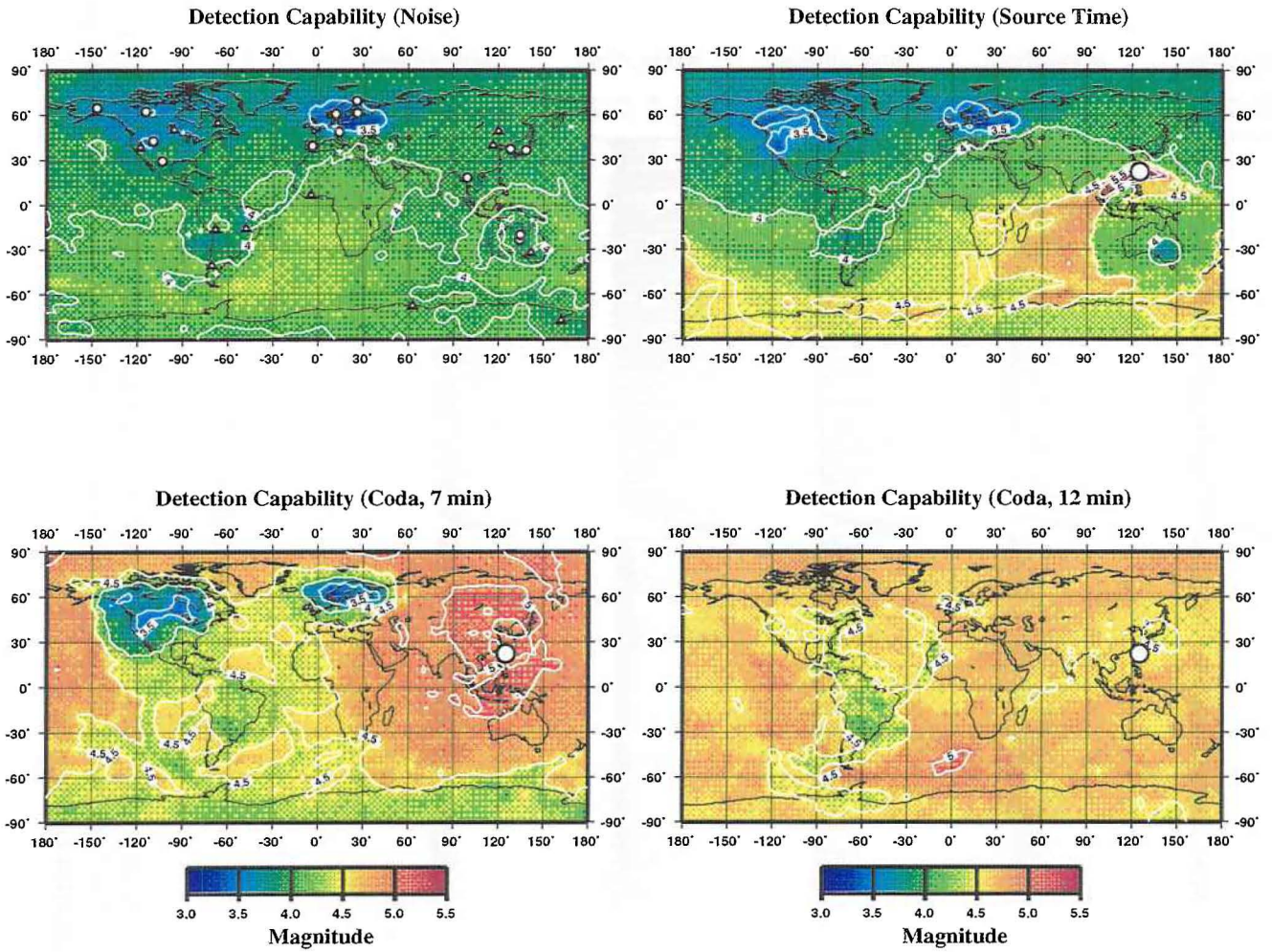

Fig. 7.1.5. Snapshots of the global detection capability display before and during a large earthquake. At the time of the earthquake, the thresholds are increased in the vicinity of the epicenter. After about 7 minutes, the threshold increases in many parts of the world, except that the P-wavefront from the earthquake has not yet reached northern Europe and North America. After 12 minutes, there is a threshold increase globally.

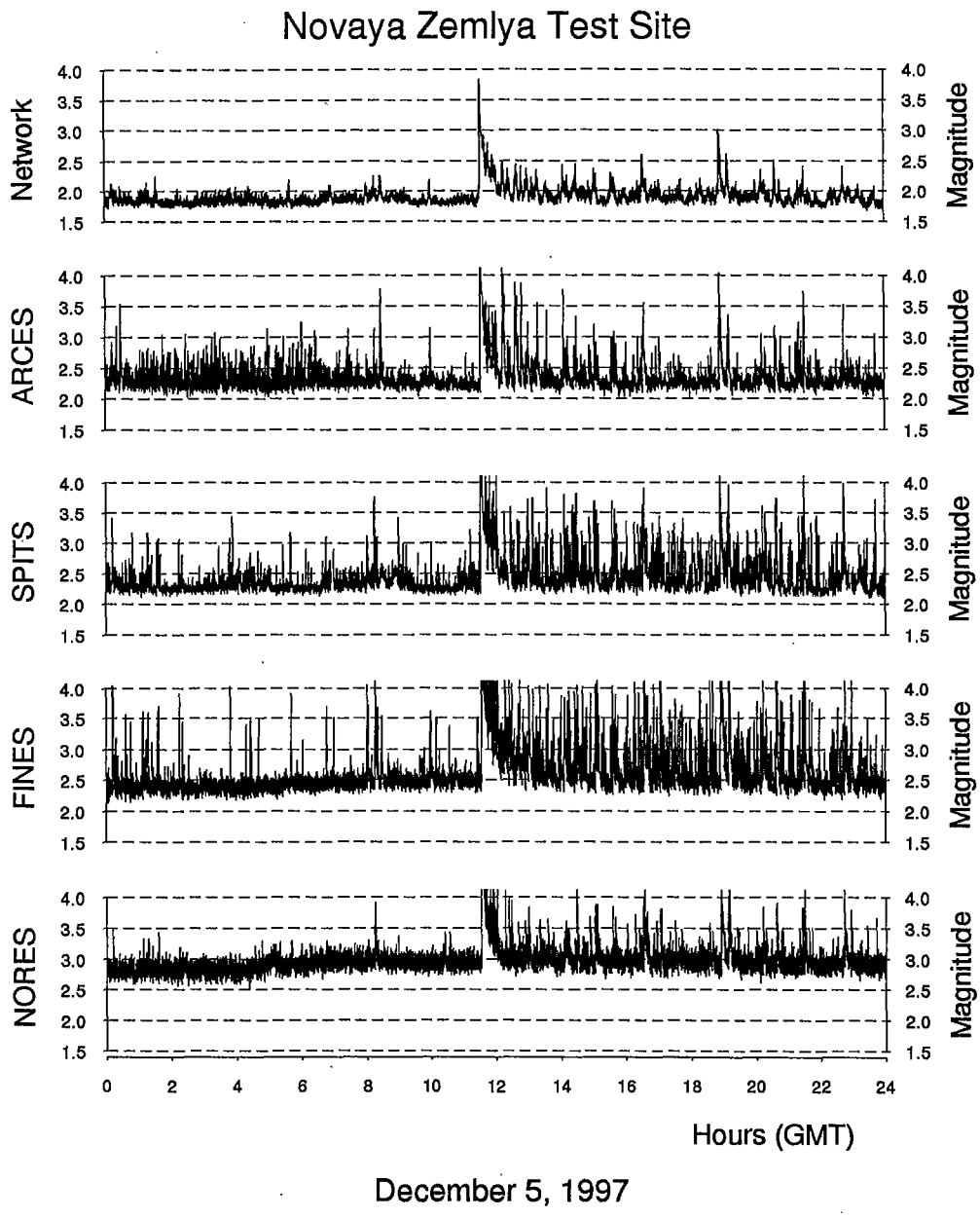

Fig. 7.1.6. Example of site-specific threshold display of the Novaya Zemlya test site for the day 5 December 1997, during which a large earthquake occurred in the Kamchatka Peninsula. See text for detailed explanation.

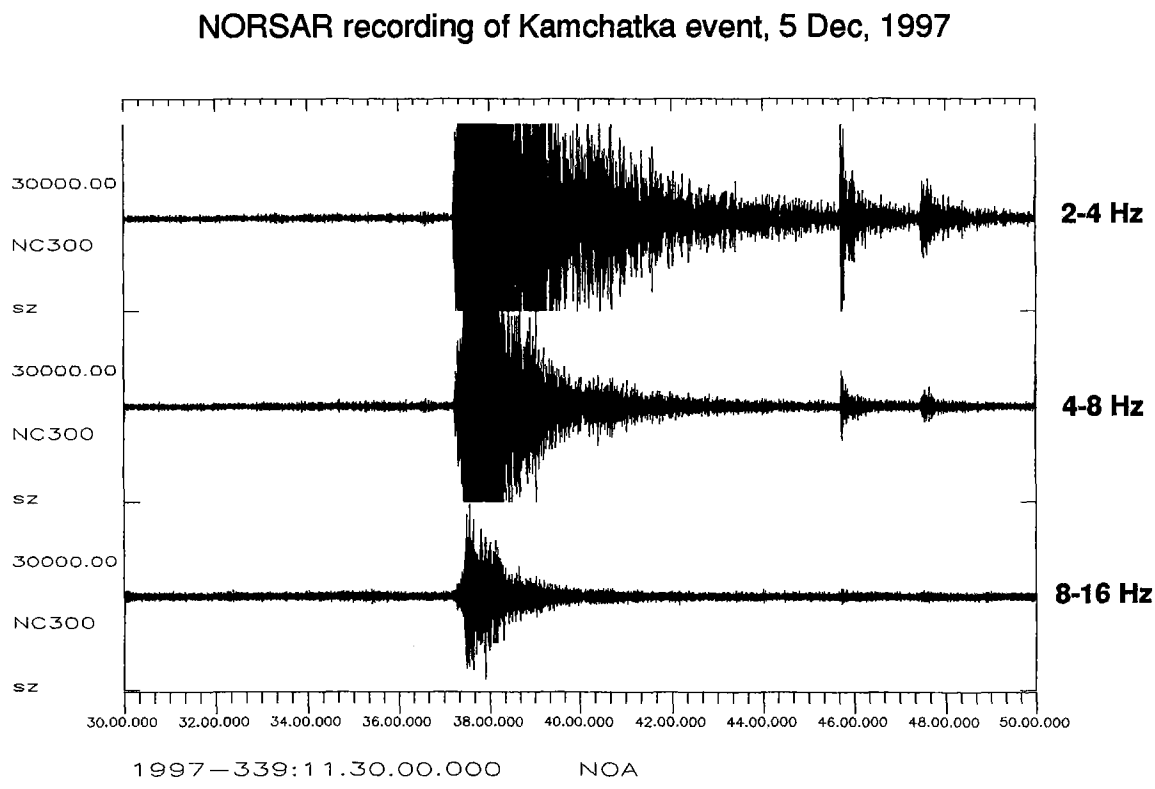

Fig. 7.1.7. Earthquake coda pattern as a function of filter frequency for the Kamchatka earthquake on 5 December 1997. The data, which have been "clipped" in the plot for illustration purposes, are from the NORSAR array, located at a teleseismic distance from the event. Note the significantly faster decrease in the coda level at the highest frequencies. Also note that the two aftershocks seen clearly on the low-frequency top trace are essentially invisible in the highest frequency band.